Long term efficacy and fate of a right ventricular outflow tract replacement using a novel developed material with optimized biodegradation and elasticity

Kazuro L Fujimoto[a,*,1], Aika Yamawaki-Ogata[a,1], Yuji Narita[a], Akihiko Usui[a], Koichiro Uto[b, c], and Mitsuhiro Ebara[b]

a Department of Cardiac Surgery, Nagoya University Graduate School of Medicine, Nagoya, Japan

b International Center for Materials Nanoarchitectonics (MANA), National Institute for Materials Science (NIMS)

c PRIME, Japan Agency for Medical Research and Development (AMED)

*Corresponding author. Department of Cardiac Surgery, Nagoya University Graduate School of Medicine, 65 Tsurumai-cho, Showa-ku, Nagoya, Aichi 466-8550, Japan. Tel: +81-52-744-2376; fax: +81-52-744-2383; e-mail: fujimotokl@med.nagoya-u.ac.jp (Fujimoto KL).

[1]Equal contributors

ABSTRACT

For decades, researchers have investigated the ideal material for clinical use in the

cardiovascular field. Several substitute materials are used clinically, but each has drawbacks. Recently we developed poly(e-caprolactone-co-D,L-lactide) (P(CL-DLLA)) polymers with optimized biodegradation and elasticity by adjusting the CL/DLLA composition, and used these polymers in right ventricular outflow tract (RVOT) replacement to evaluate long-term efficacy and outcomes. This P(CL-DLLA) material was processed into a circular patch and used to replace a surgical defect in the RVOT of adult rats. Control rats were implanted with expanded polytetrafluoroethylene (ePTFE). Histologic evaluation was performed at 8, 24, and 48 weeks post-surgery. All animals survived the surgery with no aneurysm formation or thrombus. In all periods, ePTFE demonstrated fibrous tissue. In contrast, at 8 weeks P(CL-DLLA) showed infiltration of macrophages and fibroblast-like cells into the remaining material. At 24 weeks, P(CL-DLLA) was absorbed completely, and muscle-like tissue was present with positive staining for α-sarcomeric actinin and cTnT. At 48 weeks, the cTnT-positive area had increased. The P(CL-DLLA) with optimized elasticity and biodegradation induced cardiac regeneration throughout the 48-week study period. Future application of this material as a cardiovascular scaffold seems promising.

Keywords:

biodegradable polymer, elasticity, cardiac regeneration, myofibroblast, endothelization, vascularization

1. Introduction

Some synthetic materials, such as polyethylene terephthalate fabric (DACRON) and expanded polytetrafluoroethylene (ePTFE, e.g., Gore-Tex or IMPRA), are commonly used for reconstruction of tissue deficiencies in cardiovascular surgery. These materials are not clinically ideal since each has drawbacks, for instance unsuitable mechanical properties for cardiac tissue, lack of biodegradation resulting in lack of native tissue growth, and risks of calcification and infection.

Previously, we reported that applying a cardiac patch made of biodegradable polyester urethane urea (PEUU) onto an infarcted area could prevent further cardiac dilation and preserve cardiac function after myocardial infarction, due to the material's suitable elasticity and strength [1-3]. Further, this material induced muscle cellularization in which the cells had characteristics of early cardiomyocytes, contributing to cardiac regeneration. Unfortunately, PEUU has not yet been approved by the US Food and Drug Administration (FDA) for clinical usage.

We have focused on polylactic acid (PLA), poly-ε-caprolactone (PCL), and polyglycolic acid (PGA), which have already been widely used clinically in the construction of artificial bone, tendon, skin, and sutures, and are expected to be utilized in the cardiovascular field. Our objective is to develop a biodegradable material with suitable mechanical properties for cardiovascular reconstruction and to apply this

material to cardiac tissue in vivo to prove its long-term efficacy.

To create the cardiac biomaterial, we used four-armed poly(ε-caprolactone-co-D,L-lactide) (i.e., P(CL-DLLA)), which was reported in previous papers [4-6]. In general, PCL and PLA are quite mechanically rigid; however, the elasticity of our P(CL-DLLA) material has been tuned for tissue compatibility and biodegradability [6]. We were able to use this tunable material platform in novel tissue-engineering scaffolds for nerve generation, spheroid culture, and the creation of biomaterials for cancer therapy [7-9].

In this study, we optimized the material properties of P(CL-DLLA) for use as a novel cardiac patch. The right ventricular outflow tract (RVOT) in rats was replaced with P(CL-DLLA), and the RVOT material was then examined in terms of degradation, angiogenesis, and endothelium and tissue formation after implantation periods of 8, 24, and 48 weeks. It was thought that the endpoint of 48 weeks would demonstrate the fate of the implanted biomaterial. This is the first study to report such long-term observation of biodegradable material in the heart.

2. Materials and methods

2.1. Experimental animals

Adult male Sprague-Dawley rats (Japan SLC, Inc. Shizuoka, Japan) weighing 300 g to 350 g were used for the RVOT replacement procedure. The research protocol

81 followed the National Institutes of Health guidelines for animal care and was approved
82 by the Institutional Animal Care and Use Committee of the Animal Experiment
83 Advisory Committee of the Nagoya University School of Medicine.
84
85 *2.2. Mechanical properties of P(CL-DLLA)*
86 Briefly, four-armed P(CL-DLLA) was synthesized by ring-opening polymerization
87 of CL and DLLA from terminal hydroxyl groups of pentaerythritol using tin octanoate
88 as a catalyst [7, 8]. Two types of the copolymer were also synthesized by adjusting the
89 CL/DLLA ratio to 80/20 and 60/40 (mol%). The ratio of CL/DLLA was confirmed by
90 1H NMR. The obtained copolymers were then reacted with acryloyl chloride to
91 introduce vinyl groups at the end chains. The end-functionalized macromonomers were
92 dissolved in xylene (50 wt%) and 2 wt% BPO was added. The macromonomer solution
93 was placed between two glass plates with a 4 cm x 4 cm Teflon spacer of 0.5 mm. The
94 glass plates were put in an oven at 80 °C for 3 h. The polymer was detached from the
95 glass plates and purified by immersion in a large amount of acetone. P(CL-DLLA) was
96 obtained after drying under reduced pressure. P(CL-DLLA) was characterized by tensile
97 testing (EZ-S500N, SHIMADZU, Kyoto, Japan) with a thermo-chamber that allowed
98 the temperature-dependent mechanical properties of samples to be determined. The
99 tensile tests were carried out at an elongation rate of 10 mm min-1 at 25 °C and 37 °C,
100 and the elastic modulus was calculated from the initial slope of the stress–strain curve.

For the cyclic test, a single cyclic load was applied with a strain amplitude that was gradually increased by 50% every cycle; the loading and unloading speeds were 10 mm min-1 at 25 °C until the test specimen failed. The morphology of the P(CL-DLLA) which was thread a surgical suture was observed by scanning electron microscopy (SEM; JCM-5000, JEOL).

2.3. P(CL-DLLA) or ePTFE implantation for ROVT reconstruction

The surgical procedure was based on the method previously reported by Sakai and colleagues [10]. Briefly, the heart was exposed through median sternotomy and a purse-string suture was placed in the RVOT free wall with 7-0 polypropylene to form a perimeter with a diameter greater than 6 mm (Ethicon, Somerville, NJ). Suture ends were passed through a 26-gauge plastic vascular cannula (TERUMO, Tokyo, Japan) and a tourniquet was applied and tightened. The RVOT wall inside the purse-string stitching was then distended and resected to create a defect just under 6 mm in diameter. Six-mm-diameter P(CL-DLLA) or ePTFE (GORE-TEX cardiovascular patch, W. L. Gore & Associates, Inc., NY, USA) was sutured along the margin of the purse-string suture with an over-and-over method with 7-0 polypropylene to cover the defect. The tourniquet was then released and the purse-string suture was removed, leaving a whole-wall-thickness defect just under 6 mm in diameter covered by the materials. The chest incision was closed in layers with running sutures of 4-0 Vicryl (Ethicon).

121 At each scheduled explant time point (8, 24, and 48 weeks), animals were
122 administered 500 units of heparin under anesthesia with 3% isoflurane (FUJIFILM
123 Wako Pure Chemical Co., Osaka, Japan) and were then euthanized (n = 9 per group) by
124 intravenous injection of an overdose of KCL solution. The heart was harvested and
125 frozen in OCT compound, which was pre-fixed in 4% paraformaldehyde for 48 h at
126 4 °C and gradually dehydrated in 10%, 15%, or 20% sucrose buffer overnight at 4 °C.
127
128 *2.4. Histology and immunohistochemistry*
129 The frozen heart tissue was serially cryosectioned into 10-μm-thick specimens and
130 processed for Masson trichrome or immunohistochemical evaluation. Specimens for
131 immunohistochemistry were activated with HistoVT One (Nakalai Tesque, Kyoto,
132 Japan) antigen solution for 20 min at 70 °C. Slides were then reacted with antibodies
133 against α-sarcomeric actinin (mouse monoclonal 1:50, Abcam), α-smooth muscle actin
134 (α-SMA; rabbit polyclonal 1:500, mouse monoclonal 1:100, Abcam), von Willebrand
135 factor (vWF; rabbit polyclonal 1:100, Abcam), CD11b (rabbit polyclonal 1:200, Novus
136 Biologicals, Centennial, CO, USA), or cardiac troponin T (cTnT; rabbit polyclonal
137 1:400, Abcam) overnight at 4 °C. Secondary antibodies were Alexa Fluor
138 488-conjugated antibody (anti-mouse or anti-rabbit IgG (H+L), 1:5000, Cell Signaling,
139 Danvers, MA, USA) and Alexa Fluor 546-conjugated antibody (anti-rat or anti-rabbit
140 IgG (H+L), 1:5000, Cell Signaling). Nuclei were stained with 4′,6-diamidino-2-

phenyindole, DAPI Fluoromount-G (SouthernBiotech, Birmingham, AL, USA).

Sections were also examined for the formation of a fibrous capsule around the materials and observed with an FSX100 microscope (Olympus, Tokyo, Japan). For the measurement of cTnT-positive areas, blood vessel density, and the number of CD11b-positive cells at each replacement site, excluding autologous tissue, two different sample sections were quantified by Image J software (NIH, Bethesda, MD, USA). Vessels were identified as tubular structures that stained positively for vWF.

2.5. Statistical analysis

Statistical significance among the groups was determined by a one-way factorial analysis of variance (ANOVA) using GraphPad Prism for Mac (Version 6, San Diego, CA, USA). Experimental results are expressed as mean ± S.D.

3. Results

3.1. Characterization of P(CL-DLLA)

Figure 1a shows the stress-strain curve of crosslinked P(CL-DLLA). The curve with a CL/DLLA ratio of 80/20 was strongly temperature-dependent, and the elastic moduli were 76.5 MPa at 25 °C and 307 kPa at 37 °C, respectively. On the other hand, the curve with a CL/DLLA ratio of 60/40 showed polymeric, rubber-like stress-strain curves, with elastic moduli of 241 kPa at 25 °C and 218 kPa at 37 °C, respectively.

Figure 1b shows a photograph of the crosslinked P(CL-DLLA) with a CL/DLLA ratio of 60/40. The P(CL-DLLA) thickness estimated from the cross-sectional image was approximately 0.38 mm, which was almost equivalent to that of ePTFE (0.4 mm) (Fig. 1c), and the P(CL-DLLA) had a smooth surface (Fig. 1d). A temperature-independent mechanical property of P(CL-DLLA) with a CL/DLLA ratio of 60/40 was observed, suggesting its amorphous nature. The cyclic tensile test, a single cyclic load was applied with a strain amplitude that was gradually increased by 50% every cycle, showed that The P(CL-DLLA) was failed at 1050% strain, indicating the material's super-elastic nature (Fig. 1e). On the other hand, the result of the cyclic tensile test for P(CL-DLLA) with a CL/DLLA ratio of 80/20 showed more a plastic-like nature, with an asymmetric curve similar to that of ePTFE (data not shown).

Figure 2 shows that the P(CL-DLLA) with a CL/DLLA ratio of 60/40 returned to its original form after a suture was passed through it (Fig. 2a). The morphologies of the holes made in the P(CL-DLLA) and ePTFE were not significantly different, as shown in Fig. 2b. On the other hand, when the suture was removed, the hole in the ePTFE remained open while the P(CL-DLLA) returned to its original state (Fig. 2c).

3.2. Intra- and postoperative courses

In term of surgical handling, both the P(CL-DLLA) with a CL/DLLA ratio of 80/20 and the ePTFE were stiff and difficult to penetrate with the suture needle. On the other

hand, P(CL-DLLA) with a CL/DLLA ratio of 60/40 showed excellent surgical handling and hemostasis, and no dehiscence during and after the continuous 7-0 prolene suture. There were no postoperative deaths throughout the 48-week study period, and no thrombosis occurred in either surgical group. In addition, neither group showed any dehiscence or aneurysm formation at the implanted site. The heart surfaces in both surgical groups were covered in connective tissue (Fig. 3).

3.3. Histological observations

Histological sections were stained with hematoxylin and eosin and Masson trichrome. As shown in Fig. 4, the ePTFE (Fig. 4a-f) and P(CL-DLLA) (Fig. 4g, j) groups at 8 weeks demonstrated inflammatory cells infiltration of the surrounding layered fibrous tissue. No changes were observed in the ePTFE group throughout 48 weeks. In contrast, at 8 weeks the P(CL-DLLA) group showed remaining P(CL-DLLA) as indicated by arrows, as well as infiltration of inflammatory cells and fibroblast-like cells (Fig. 4g, j). At 24 weeks, the foreign body reaction had ended and the P(CL-DLLA) was completely absorbed (Fig. 4h, k). In addition, muscle-like tissue and collagen synthesis appeared at 24 and 48 weeks (Fig. 4i, l). Hematoxylin and eosin staining indicated that there was no calcification in any of the samples.

3.4. Expression patterns of α-sarcomeric actinin, α-SMA, cTnT, vWF, and CD11b in the

P(CL-DLLA) group

In immunohistochemical analysis of α-sarcomeric actinin and α-SMA at 8 weeks, the P(CL-DLLA) contained many cells with positive for α-SMA (Fig. 5a-c). At 24 weeks, immature α-sarcomeric actinin-positive cells appeared and tubular structures that stained positively for α-SMA (Fig. 5d-f). At 48 weeks, abundant α-sarcomeric actinin-positive cells were observed within the muscle bundles (Fig. 5g-i).

To confirm cTnT expression patterns, each section was co-stained with α-sarcomeric actinin and the cardiac-specific protein cTnT. No tissues expressing both proteins were seen at 8 weeks (Fig. 6a-c), while such tissues had begun to develop at 24 weeks (Fig. 6d-f) and were widespread at 48 weeks (Fig. 6g-i). The cTnT-positive area in the replacement site increased gradually as time passed (Fig. 6j; 8 weeks, 5.6 ± 3.3 mm^2; 24 weeks, 219.2 ± 165.8 mm^2; 48 weeks, 416.6 ± 275.5 mm^2). There was a significant difference between each pair of time points (8 vs 24 weeks, $p < 0.01$; 8 vs 48 weeks, $p < 0.001$; 24 vs 48 weeks, $p < 0.01$).

For assessment of endothelialization and vascularization, samples were stained with vWF as shown in Fig. 7. The P(CL-DLLA) group at each time point after implantation showed complete endocardial endothelialization. Vascularization was observed at each time point, and the maximum blood vessel density occurred at 8 weeks (Fig. 7j; 8 weeks, 230.1 ± 81.4 /mm^2; 24 weeks, 119.8 ± 39.9 /mm^2; 48 weeks, 120.2 ± 42.5 /mm^2; 8 vs 24 weeks, $p < 0.001$; 8 vs 48 weeks, $p < 0.001$).

To identify infiltrating inflammatory cells, the sections were stained with CD11b. Many CD11b-positive cells infiltrated the P(CL-DLLA), and their number decreased over time (Fig. 8j; 8 weeks, 23.3 ± 7.9 %; 24 weeks, 8.0 ± 3.4 %; 48 weeks, 6.2 ± 1.7 %; 8 vs 24 weeks, $p < 0.001$; 8 vs 48 weeks, $p < 0.001$).

4. Discussion

We previously developed a novel PCL-based material with tunable thermal and mechanical properties as well as shape memory ability [8, 11, 12]. Despite being composed of only crosslinked P(CL-DLLA), this biodegradable polymeric material possesses high elasticity and strength. We already utilized this material platform as a scaffold for nerve regeneration and spheroid cell culture [7, 8]. Given this material's superior characteristics, we assumed it could serve as an elastic patch for tissue reconstruction in the cardiovascular system, but its in vivo biocompatibility, biodegradability, and clinical potential remained unknown. Thus, we designed a new P(CL-DLLA) material with different CL/DLLA composition for in vivo cardiac patch application. The material's physical appearance, such as its surface morphology and thickness, as well as its thermal and mechanical properties, were optimized by changing the CL/DLLA ratio. A dramatic improvement in the material's characteristics, including its mechanical properties and surgical handling, was achieved by small change (~20 mol%) in the CL/DLLA ratio. The optimized material, crosslinked P(CL-DLLA) with a

CL/DLLA ratio of 60/40, had tissue-compatible, super-elastic nature (< 300 kPa) showing elastic behavior over 1000% strain, and we therefore anticipated that it would be useful as a material for a cardiac patch.

The results of this study showed that when this novel, optimized P(CL-DLLA) was used to repair a surgical defect in the RVOT, it achieved good initial hemostasis and surgical handling, gradually degraded as cell migration and vascularization occurred, and led to formation of completely new tissue by self-organization of the host cardiac muscle-like cells. Importantly, this study specifically involved long-term observation that has not been detailed in other reports.

When ePTFE was implanted in the RVOT area, it remained surrounded by loose fibrous tissue for the entire 48-week study, and the repaired area was presumably too stiff to serve as a functional heart wall. On the other hand, at 8 weeks the right ventricle wall repaired with P(CL-DLLA) demonstrated marked cell migration and was found to express α-SMA and CD11b. At all time points, the P(CL-DLLA) showed endothelialization with vWF-positive cells as well as abundant vascularization with co-expression of α-SMA and vWF, without any evidence of thrombosis. At 24 weeks, the P(CL-DLLA) had completely degraded and was replaced by a muscle layer consisting of cells that co-expressed α-sarcomeric actinin and cTnT, possibly representing cardiomyocytes. Notably, at 48 weeks this muscle tissue was still present and the number of cTnT-positive cells had increased. It is speculated that the substrate

stiffness and strain induced differentiation or de-differentiation (reverse-remodeling) of the myofibroblast phenotype [13-15]. Further investigation is necessary to elucidate the mechanism of this cardiac regeneration.

The elastic modulus values of native adult rat hearts have been reported to range from 11.9 to 46.2 kPa (mean value of 25.6 kPa) [16], while that of our material in an in vitro experiment was 218 kPa at 37 °C, which was sufficient for mechanical reinforcement. According to Hazeltine et al [17], however, a 50-kPa elastic modulus is preferred for cardiogenesis. It should be taken into consideration that in vivo, the replacement material is degraded not only through hydrolysis but also through macrophage phagocytosis. Significant tensile strength is required in the high-pressure environment of the heart while the material is being replaced by new tissue. The P(CL-DLLA) in this study functioned well clinically given the fact that no rats died even over the long 48-week observation period. As shown in Fig. 4, the P(CL-DLLA) in vivo was gradually fragmented, and this fragmentation might participate the change of mechanical properties. In fact, our previous study indicated that the microchannel structure of the P(CL-DLLA) scaffold affected its mechanical properties [7]. This report shows that since the elastic modulus of P(CL-DLLA) gradually decreased as a result of fragmentation in vivo, it might eventually be suitable to facilitate transformation into differentiation of cardiomyocytes from myofibroblasts .

In this study, we optimized the unique characteristics of P(CL-DLLA), including its

elasticity and biodegradability, and thereby induced muscle tissue regeneration. At the same time, several issues should be considered in further studies. First, the beneficial effects of RVOT remodeling were observed in a rat model. Further exploration in a large animal model is needed, where changes in the replaced RVOT area and the volume of RVOT remodeling more closely approximate the clinical setting. Second, the origin of the myofibroblasts that appeared in the replaced RVOT wall was unknown. Histological sections did not clearly indicate that this tissue migrated from the healthy periphery of the heart. Employment of a marrow ablation model using a chimera with fluorescently labeled reconstituted marrow would permit investigation of these cells' origin and differentiation. Finally, this cardiac regeneration usig P(CL-DLLA) could be more beneficial for left ventricular infarction. In our previous studies, cardiac function after infarction could be preserved by covering the infarcted area with PEUU or by injecting poly(NIPAAm-co-AAc-co-HEMAPTMC) hydrogel [1-3, 18]. Even though further optimization is needed for a system with higher pressure than that of the right ventricle, it is encouraging that "off-the-shelf" P(CL-DLLA) consisting of FDA-approved material is quite useful in various clinical settings, especially for preventing the need for biological treatment.

Conclusion

This study evaluated the potential of a novel cardiac patch made of biodegradable

cross-linked P(CL-DLLA) polymers. This patch had unique mechanical properties, particularly optimized elasticity, that made it suitable for long-term, in vivo RVOT repair. The P(CL-DLLA) successfully induced new tissue growth during the initial 24-week period, including differentiation of cardiomyocytes from myofibroblasts, endocardial endothelialization, and vascularization, and the new tissue was maintained throughout the 48-week study. P(CL-DLLA) warrants further investigation for the reconstruction of tissue deficiencies in cardiovascular surgery.

Declaration of competing interest

The authors declare no conflicts of interest.

Acknowledgements

The authors thank the Division for Experimental Animals, Nagoya University Graduate School of Medicine, for managing the animals used in this study. The authors would like to thank the Division for Medical Research Engineering, Nagoya University Graduate School of Medicine, for the use of a cryomicrotome (Leica) and FSX100 microscope (Olympus).

Funding

This study was supported in part by a Grant-in-Aid for Science Research (No.

26462086) from the Ministry of Education, Culture, Sports, Science, and Technology of Japan.

References

[1] K.L. Fujimoto, K. Tobita, W.D. Merryman, J. Guan, N. Momoi, D.B. Stolz, M.S. Sacks, B.B. Keller, W.R. Wagner, An elastic, biodegradable cardiac patch induces contractile smooth muscle and improves cardiac remodeling and function in subacute myocardial infarction, J. Am. Coll. Cardiol. 49 (2007) 2292-2300. https://doi.org/10.1016/j.jacc.2007.02.050

[2] K.L. Fujimoto, J. Guan, H. Oshima, T. Sakai, W.R. Wagner, In vivo evaluation of a porous, elastic, biodegradable patch for reconstructive cardiac procedures, Ann. Thorac. Surg. 83 (2007) 648-654. https://doi.org/10.1016/j.athoracsur.2006.06.085

[3] K.L. Fujimoto, K. Tobita, J. Guan, R. Hashizume, K. Takanari, C.M. Alfieri, K.E. Yutzey, W.R. Wagner, Placement of an elastic biodegradable cardiac patch on a subacute infarcted heart leads to cellularization with early developmental cardiomyocyte characteristics, J. Card. Fail. 18 (2012) 585-595. https://doi.org/10.1016/j.cardfail.2012.05.006

[4] T. Aoyagi, F. Miyata, Y. Nagase, Preparation of Cross-Linked Aliphatic Polyester and Application to Thermoresponsive Material, J. Control. Release. 32 (1994) 87-96.

[5] H. Miyasako, K. Yamamoto, A. Nakao, T. Aoyagi, Preparation of cross-linked

poly[(epsilon-caprolactone)-co-lactide] and biocompatibility studies for tissue engineering materials, Macromol. Biosci. 7 (2007) 76-83. https://doi.org/10.1002/mabi.200600188

[6] T. Muroya, K. Yamamoto, T. Aoyagi, Degradation of cross-linked aliphatic polyester composed of poly(epsilon-caprolactone-co-D,L-lactide) depending on the thermal properties, Polym. Degrad. Stabil. 94 (2009) 285-290. https://doi.org/10.1016/j.polymdegradstab.2008.12.014

[7] K. Uto, T. Muroya, M. Okamoto, H. Tanaka, T. Murase, M. Ebara, T. Aoyagi, Design of super-elastic biodegradable scaffolds with longitudinally oriented microchannels and optimization of the channel size for Schwann cell migration, Sci. Technol. Adv. Mater. 13 (2012) 064207. https://doi.org/10.1088/1468-6996/13/6/064207

[8] K. Uto, S.S. Mano, T. Aoyagi, M. Ebara, Substrate Fluidity Regulates Cell Adhesion and Morphology on Poly(epsilon-caprolactone)-Based Materials, Acs. Biomater. Sci. Eng. 2 (2016) 446-453. https://doi.org/10.1021/acsbiomaterials.6b00058

[9] S.S. Mano, K. Uto, T. Aoyagi, M. Ebara, Fluidity of biodegradable substrate regulates carcinoma cell behavior: A novel approach to cancer therapy, AIMS. Mater. Sci. 3 (2016) 66-82. https://doi.org/10.3934/matersci.2016.1.66

[10] T. Sakai, R.K. Li, R.D. Weisel, D.A. Mickle, E.T. Kim, Z.Q. Jia, T.M. Yau, The fate of a tissue-engineered cardiac graft in the right ventricular outflow tract of the rat, J. Thorac. Cardiovasc. Surg. 121 (2001) 932-942.

https://doi.org/10.1067/mtc.2001.113600

[11] K. Uto, T. Aoyagi, C.A. DeForest, A.S. Hoffman, M. Ebara, A Combinational Effect of "Bulk" and "Surface" Shape-Memory Transitions on the Regulation of Cell Alignment, Adv. Healthc. Mater. 6 (2017). https://doi.org/10.1002/adhm.201601439

[12] K. Uto, M. Ebara, T. Aoyagi, Temperature-responsive poly(epsilon-caprolactone) cell culture platform with dynamically tunable nano-roughness and elasticity for control of myoblast morphology, Int. J. Mol. Sci. 15 (2014) 1511-1524. https://doi.org/10.3390/ijms15011511

[13] A.K. Schroer, W.D. Merryman, Mechanobiology of myofibroblast adhesion in fibrotic cardiac disease, J. Cell. Sci. 128 (2015) 1865-1875. https://doi.org/10.1242/jcs.162891

[14] P. Kim, N. Chu, J. Davis, D.H. Kim, Mechanoregulation of Myofibroblast Fate and Cardiac Fibrosis, Adv. Biosyst. 2 (2018). https://doi.org/10.1002/adbi.201700172

[15] C. Godbout, L. Follonier Castella, E.A. Smith, N. Talele, M.L. Chow, A. Garonna, B. Hinz, The mechanical environment modulates intracellular calcium oscillation activities of myofibroblasts, PLoS One. 8 (2013) e64560. https://doi.org/10.1371/journal.pone.0064560

[16] B. Bhana, R.K. Iyer, W.L. Chen, R. Zhao, K.L. Sider, M. Likhitpanichkul, C.A. Simmons, M. Radisic, Influence of substrate stiffness on the phenotype of heart cells, Biotechnol. Bioeng. 105 (2010) 1148-1160. https://doi.org/10.1002/bit.22647

[17] L.B. Hazeltine, M.G. Badur, X.Lian, A Das, W. H, S.P. Palecek, Temporal Impact of Substrate Mechanics on Differentiation of Human Embryonic Stem Cells to Cardiomyocytes, Acta Biomater. 10 (2014) 604-612. https://doi.org/10.1016/j.actbio.2013.10.033

[18] K.L. Fujimoto, Z. Ma, D.M. Nelson, R. Hashizume, J. Guan, K. Tobita, W.R. Wagner, Synthesis, characterization and therapeutic efficacy of a biodegradable, thermoresponsive hydrogel designed for application in chronic infarcted myocardium, Biomaterials. 30 (2009) 4357-4368. https://doi.org/10.1016/j.biomaterials.2009.04.055

Figures

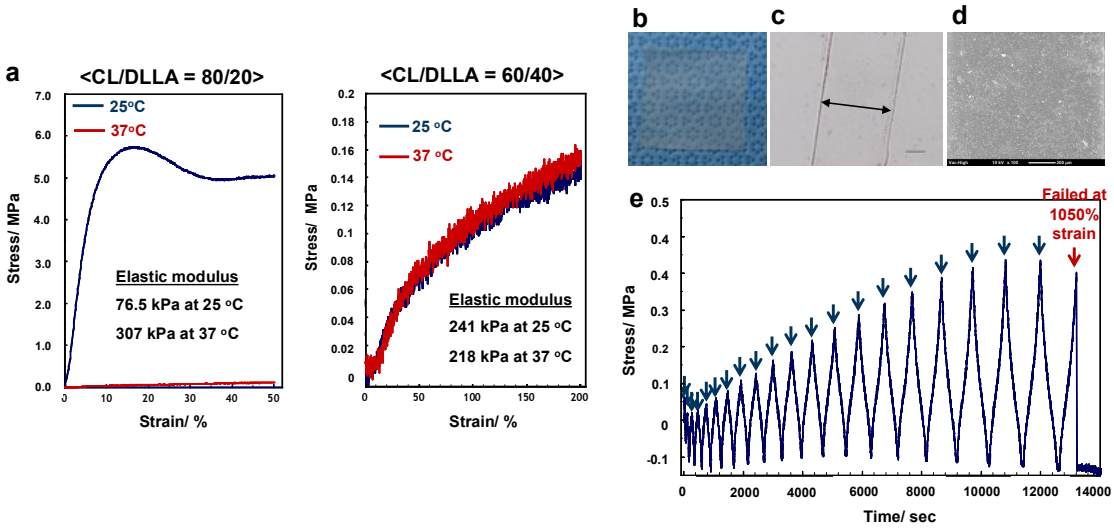

Fig. 1. Form and characterization of P(CL-DLLA). (a) Stress-strain curves of P(CL-DLLA) at 25 and 45 °C. (b) Photograph of P(CL-DLLA) with a CL/DLLA ratio

of 60/40 prepared by thermal crosslinking. (c) Cross-sectional image of P(CL-DLLA) with a CL/DLLA ratio of 60/40 observed by an optical microscope (scale bar, 100 μm). (d) Scanning electron microscopy (SEM) image of surface morphology of P(CL-DLLA) with a CL/DLLA ratio of 60/40 (scale bar, 200 μm). (e) Cyclic tensile test with a loading/unloading speed of 10 mm min-1 at 25 °C. The constant strain amplitude of 50% per cycle was applied to the P(CL-DLLA) with a CL/DLLA ratio of 60/40 until it broke.

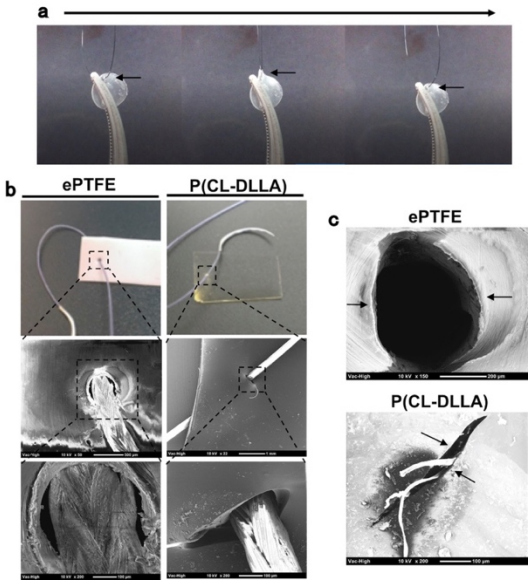

Fig. 2. Morphology of P(CL-DLLA) with a CL/DLLA ratio of 60/40. (a) Images over time before and after pulling the surgical suture threaded on the P(CL-DLLA). (b) Photographs and SEM images of the P(CL-DLLA) and ePTFE at the location of suture penetration. (c) SEM images of P(CL-DLLA) and ePTFE surfaces after suture removal.

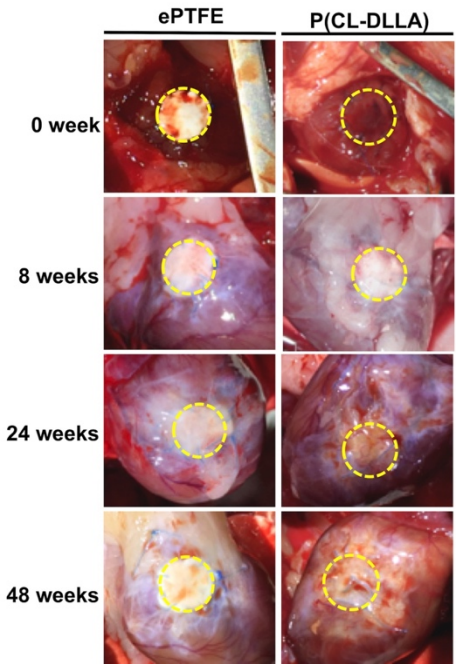

Fig. 3. RVOT repair with ePTFE or P(CL-DLLA). (a) Representative images at 0, 8, 24 and 48 weeks after RVOT repair with 6-mm-diameter P(CL-DLLA) or ePTFE.

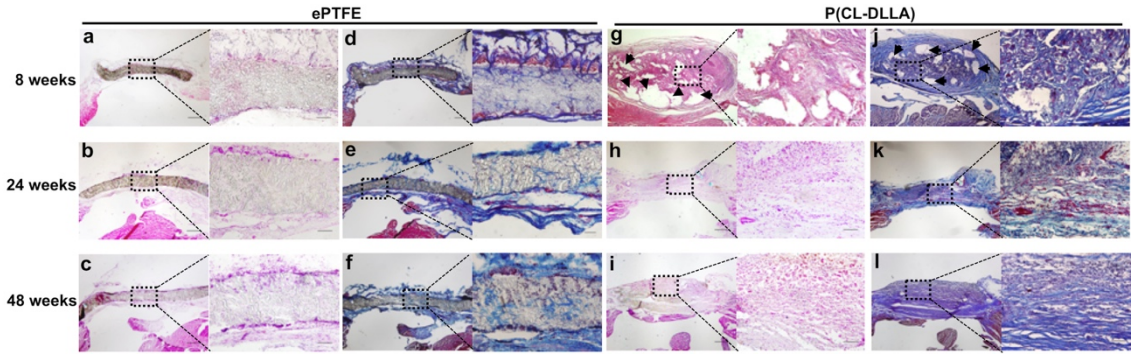

Fig. 4. Time course of the healing response after RVOT repair with ePTFE or P(CL-DLLA). Representative images of the ePTFE group at 8 weeks (a, d), 24 weeks (b, e), and 48 weeks (c, f), and the P(CL-DLLA) group at 8 weeks (g, j), 24 weeks (h, k), and 48 weeks (i, l). Samples were stained with hematoxylin and eosin staining (a-f) or Masson trichrome staining (g-l). Scale bars: 200 μm in the left images, and 50 μm in the

right images. Arrows indicate the area of remaining P(CL-DLLA).

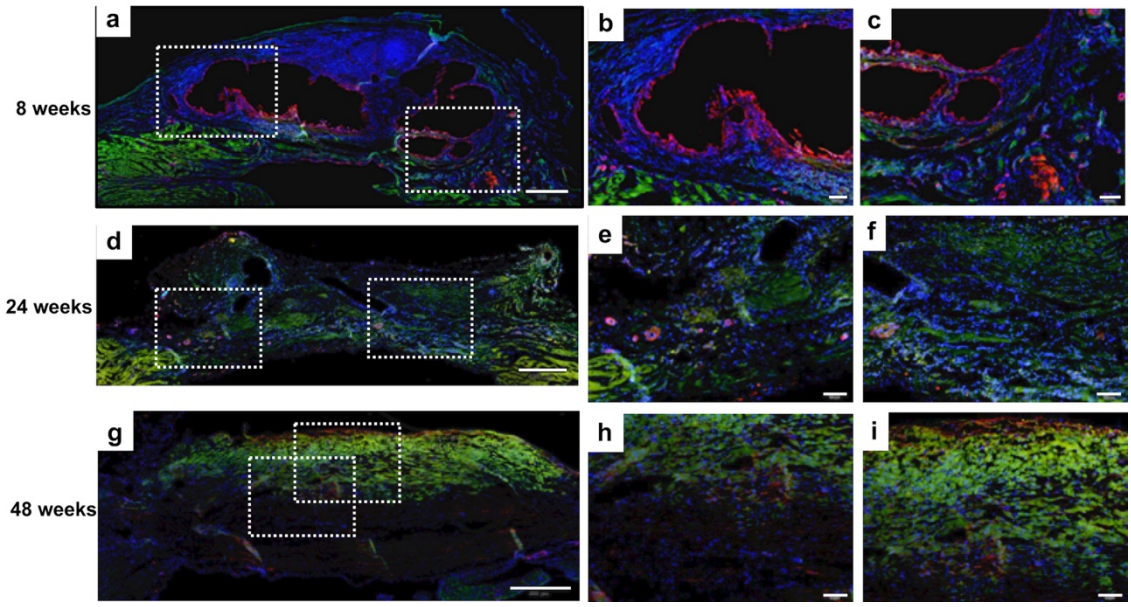

Fig. 5. Time course of immunofluorescence staining of the P(CL-DLLA) area with α-sarcomeric actinin and α-SMA. Representative images of the P(CL-DLLA) group at 8 weeks (a-c), 24 weeks (d-f), and 48 weeks (g-i). α-sarcomeric actinin staining appears green, α-SMA staining appears red, and nuclear staining appears blue. White squares indicate areas with greater magnification in the panels to the right. Scale bars: 500 μm in (a, d, g), 100 μm in (b, c, e, f, h, i).

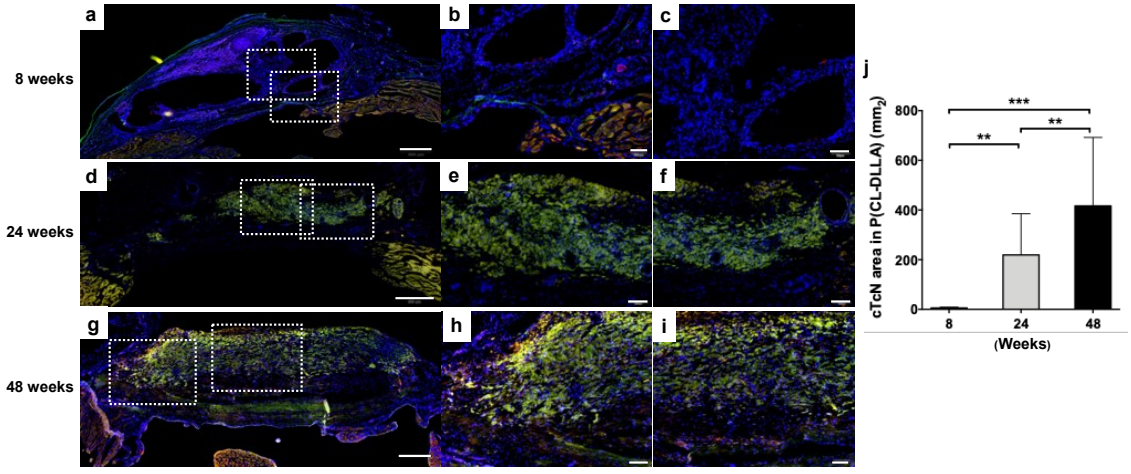

Figure 6

Fig. 6. Time course of immunofluorescence staining of the P(CL-DLLA) area with α-sarcomeric actinin and cTnT. Representative images of the P(CL-DLLA) group at 8 weeks (a-c), 24 weeks (d-f), and 48 weeks (g-i). Alpha-sarcomeric actinin staining appears green, cTnT staining appears red, and nuclear staining appears blue. White squares indicate areas with greater magnification in the panels to the right. Scale bars: 500 μm in (a, d, g), 100 μm in (b, c, e, f, h, i). (j) The cTnT-positive area in the P(CL-DLLA) repair at 8, 24, and 48 weeks. Data are means ± S.D. **p < 0.01 and ***p < 0.001 assessed by one-way ANOVA.

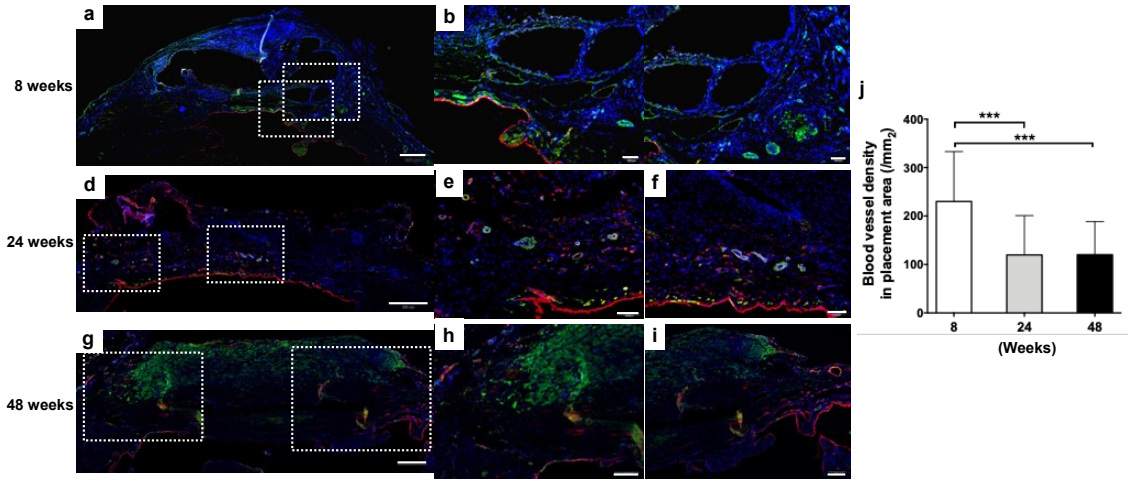

Figure 7

Fig. 7. Time course of immunofluorescence staining of the P(CL-DLLA) area with α-SMA and vWF. Representative images of the P(CL-DLLA) group at 8 weeks (a-c), 24 weeks (d-f), and 48 weeks (g-i). Alpha-SMA staining appears green, vWF staining appears red, and nuclear staining appears blue. White squares indicate areas with greater magnification in the panels to the right. Scale bars: 500 μm in (a, d, g), 100 μm in (b, c,

e, f, h, i). (j) The blood vessel density in the P(CL-DLLA) repair at 8, 24, and 48 weeks. Data are means ± S.D. ***p < 0.001 assessed by one-way ANOVA.

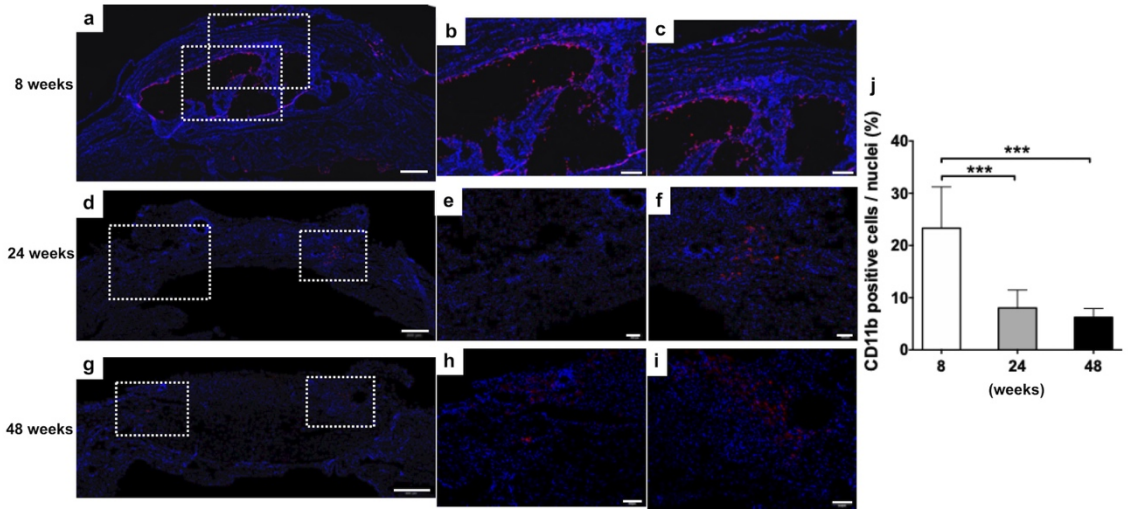

Fig. 8. Time course of immunofluorescence staining of the P(CL-DLLA) area with CD11b. Representative images of the P(CL-DLLA) group at 8 weeks (a-c), 24 weeks (d-f), and 48 weeks (g-i). CD11b staining appears red and nuclear staining appears blue. White squares indicate areas with greater magnification in the panels to the right. Scale bars: 500 μm in (a, d, g), 100 μm in (b, c, e, f, h, i). (j) The number of CD11b-positive cells in the P(CL-DLLA) repair at 8, 24, and 48 weeks. Data are means ± S.D. ***p < 0.001 assessed by one-way ANOVA.